

Combination of cationic dexamethasone derivative and STAT3 inhibitor (WP1066) for aggressive melanoma: a strategy for repurposing a phase I clinical trial drug

Samaresh Sau^{1,2} · Sujan Kumar Mondal^{1,3} · Sushil K. Kashaw⁴ · Arun K. Iyer^{2,5} · Rajkumar Banerjee^{1,3}

Received: 11 March 2017 / Accepted: 30 May 2017
© Springer Science+Business Media New York 2017

Abstract Glucocorticoid, such as dexamethasone (Dex) is often used along with chemotherapy to antagonize side effects of chemotherapy. However, sustained use of Dex frequently develops drug resistance in patients. As a strategy to re-induce drug sensitivity, we planned to modify Dex by chemically conjugating it with twin ten carbon aliphatic chain containing cationic lipid. The resultant molecule, DX10, inhibited STAT3 activation through lowering the production of IL-6. To enhance the STAT3 inhibitory effect of DX10, we used WP (a commercially available STAT3 inhibitor) along with DX10. Combination treatment of both significantly inhibited STAT3 activation when compared to either of the individual treatment. The

effect of DX10, either in combination or alone, was mediated through glucocorticoid receptor (GR), thereby repurposing the role of GR in the context of p-STAT3 inhibition-mediated cancer treatment. Cellular viability study proved the synergistic effect of WP and DX10. Further, combination treatment led to induction of early stage of apoptosis and cell cycle arrest. In vivo melanoma tumor regression study confirmed the enhanced anti-tumor activity of co-treatment over individual treatment of DX10 or WP. Thus, together our result demonstrates that DX10 may be used in combination therapy with STAT3 inhibitor like WP for combating cancer with constitutively active STAT3.

Electronic supplementary material The online version of this article (doi:[10.1007/s11010-017-3084-z](https://doi.org/10.1007/s11010-017-3084-z)) contains supplementary material, which is available to authorized users.

Samaresh Sau and Sujan Kumar Mondal have contributed equally to this work.

✉ Samaresh Sau
sausamaresh@gmail.com; samaresh.sau@wayne.edu

✉ Arun K. Iyer
arun.iyer@wayne.edu

✉ Rajkumar Banerjee
banerjee@iict.res.in; rkbanerjee@yahoo.com

¹ Biomaterials Group, CSIR-Indian Institute of Chemical Technology, Hyderabad 500 007, India

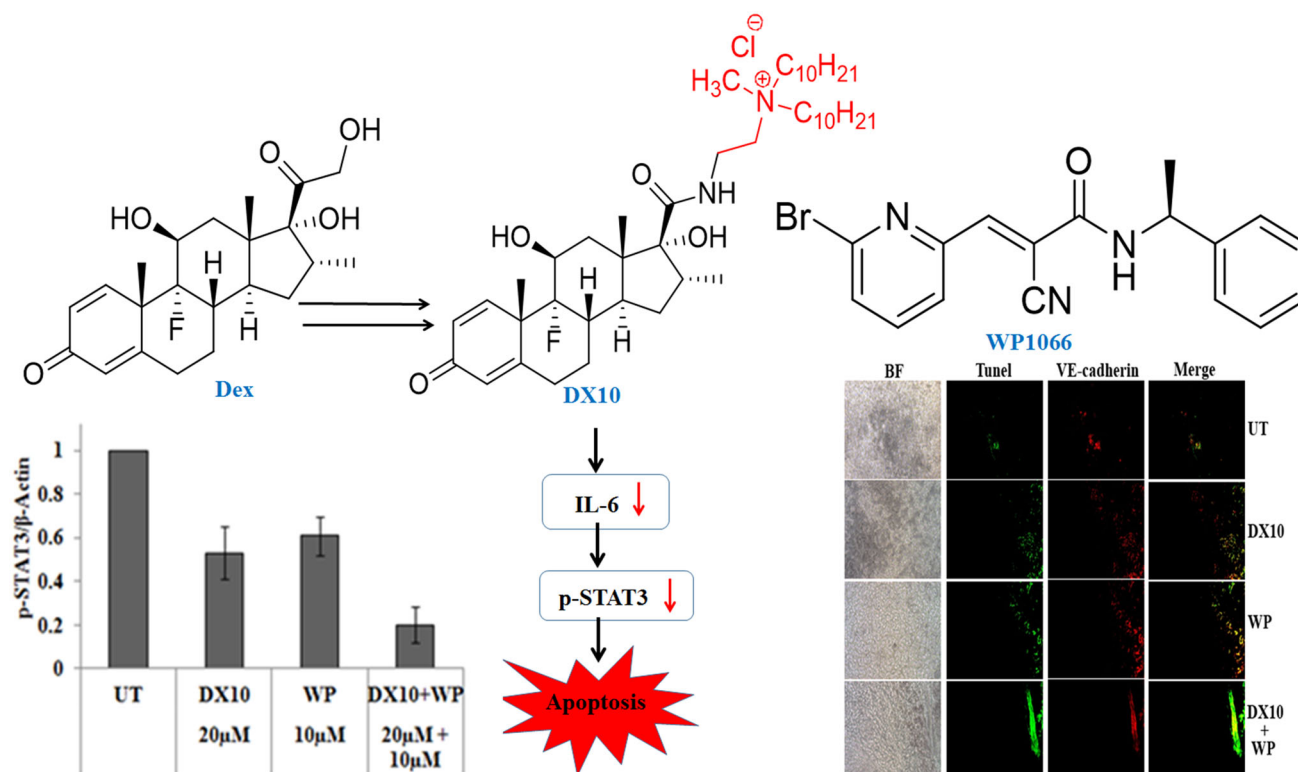
² Use-inspired Biomaterials & Integrated Nano Delivery (U-BiND) Systems Laboratory, Department of Pharmaceutical Sciences, Eugene Applebaum College of Pharmacy and Health Sciences, Wayne State University, 259 Mack Ave, Detroit, MI 48201, USA

³ Academy of Scientific and Innovative Research (AcSIR), Training and Development Complex, CSIR Campus, CSIR Road, Taramani, Chennai, Tamil Nadu 600 113, India

⁴ Department of Pharmaceutical Sciences, Dr. Harisingh Gour University, Sagar, Madhya Pradesh 470003, India

⁵ Molecular Therapeutics Program, Barbara Ann Karmanos Cancer Institute, Wayne State University, School of Medicine, Detroit, MI 48201, USA

Graphical abstract



Keywords Glucocorticoid receptor · Dexamethasone derivative · STAT3 inhibition · Drug sensitization · Repurposing WP1066

Introduction

Drug resistance in cancer cell against conventional chemotherapy is one of the most difficult challenges in oncology [1]. Cancer slowly acquires drug resistance over the course of chemotherapy depending on several factors including tumor cells' phenotypic and genotypic differences, individual disparity among patients, and origin of tumor. Among these several factors, recent development indicates that alteration in signaling pathway and genetic mutations plays critical role in developing drug resistance [2, 3]. To overcome this type of drug resistance, common combinational strategy has been preferred over conventional chemotherapy approach in which multiple drugs are simultaneously used to encounter the altered signaling pathway thereby leading to enhancement of anti-cancer efficacy [4–6].

Stimulations of signal transducer and activation of transcription 1/3/5 (STAT1/3/5) play important roles in cell division and cell growth by preventing activation of apoptosis in hematopoietic cells [7]. Overactivation of certain STAT family members, especially STAT3 leads to

formation of wide variety of malignancies including melanoma, breast cancer, epithelial cancers, multiple myeloma (MM), and different types of hematological malignancies [8–10]. Recent studies on multiple myeloma suggested that STAT3-mediated B-cell lymphoma extra-large (Bcl-xL) activation renders anti-cancer drug resistance by inhibiting Fas ligand-mediated apoptosis [11, 12]. STAT3 activities are also regulated by B-cell lymphoma (Bcl-2) protein. Thus, Bcl-2 and Bcl-xL attenuate chemotherapy-induced programmed cell death, thereby resulting in STAT3-mediated chemotherapeutic resistance in MM cells. However, activation of STAT3 by JAK kinase is monitored by IL-6 cytokine. Hence, cytokine receptor-mediated signaling via JAK kinase culminates activation of STAT3-induced anti-apoptotic and drug resistance phenotypes [13, 14]. Therefore, one can expect that inhibition of IL-6/JAK/STAT3 axis could transform drug-resistant cancer cells to drug-sensitive cells activating apoptosis-mediated cell death machinery. Thus, combination of JAK/STAT inhibitor with potent anti-cancer drug is becoming attractive target in the field of intervention chemotherapy. As for example, combination of JAK/STAT inhibitor with anti-cancer drugs (vinblastine, Adriamycin, and cisplatin) can effectively sensitize MM tumor cells, U266 by regulating Bcl-2 family proteins [14].

Dex is commonly used with other chemotherapeutic drugs to overcome the treatment-related edema, inflammation,

pain and also to combat standard chemotherapy-associated appetite, nausea, and toxic side effects [15–17]. Dex is also a frequently used chemotherapeutic drug against lymphoid-associated malignancies [18]. However, recent studies have indicated that Dex could help in acquiring drug resistance by cancer cells against standard chemotherapy through inhibiting apoptosis [14, 19]. This Dex-mediated anti-apoptotic effect is linked to the down-regulation of Caspase-9/3. Thus, treatment of Caspase-9/3 activator molecules alleviates drug sensitivity in Dex-resistance carcinomas [14]. Collectively, these observations suggest anti-apoptotic effect of Dex in chemotherapy or radiotherapy that eventually yields drug resistance in tumor patients. However, several mechanistic pathways have been identified to understand the difficulties of Dex-mediated resistance. GC, such as Dex is anyway required to alleviate toxic side effects related to chemotherapy treatment. Therefore, careful use of Dex is needed to achieve the success in combination therapy. To this end, development of new types of GCs (such as through chemical modification of Dex) and their use in combination treatment with potent anti-cancer drugs, or inhibitors would be a useful strategy for chemotherapy.

Previously, we have shown that eight carbon long cationic chain lipid conjugated Dex derivative (DX8) has promising selective anti-cancer effect [20]. DX8 exerted its anti-cancer activity by inhibiting STAT3 activation. Keeping this novel STAT3 inhibition activity of DX8 in mind, here we develop ten carbon long cationic chain conjugated Dex derivative (DX10) similar to DX8, hypothesizing that the new DX10 will also inhibit JAK/STAT3 pathway. Herein, we have synthesized and evaluated synergistic anti-cancer effect of DX10 in combination with WP [21, 22]. In this study we found that DX10 either as alone or in combination treatment inhibits JAK/STAT3 pathway by lowering IL-6 production. Apoptosis study reveals that effect of [DX10+WP] is associated with the induction of early stage of apoptosis and cell cycle arrest in different phases of cancer cell. A preclinical study in mice melanoma-based allograft model shows that [DX10+WP] significantly inhibits aggressive tumor melanoma growth. The overall study may put forward the idea that STAT3 inhibition activity of DX10 could be used along with other STAT3 inhibitors to amplify this effect and thus exhibit enhanced anti-tumor effect.

Materials and methods

Chemicals and general procedures

Dexamethasone (Dex), trypsin, EDTA, 3-(4,5-dimethylthiazol-2-yl)-2,5-diphenyltetrazoliumbromide (MTT), propidium iodide (PI), FITC-labeled annexin V, dimethyl

sulfoxide (DMSO), Dulbecco's Modified Eagle Medium (DMEM), and RPMI 1640 were purchased from Sigma Chemical Co. (St. Louis, MO). Fetal bovine serum (FBS) was purchased from Lonza, Swiss chemicals. The solvents, salts, and common reagents for synthesis were purchased either from Aldrich (Milwaukee, WI, USA) or S. D. Fine Chem (Mumbai, India). All other chemicals and reagents were purchased either from Sigma (St. Louis, MO, USA) or from Rankem Ltd. (Mumbai, India). WP1066 (WP) was purchased from Calbiochem, Merck, USA. These were used without further purification. Glucocorticoid receptor siRNA was purchased from Santa Cruz Biotech (35505) and scrambled siRNA was purchased from Qiagen. ELISA kit for IL6 was procured from eBioscience (88-7064). All molecules were characterized by ¹H NMR and/or ESI-MS. Final molecule was characterized by ESI-HRMS and ¹³C NMR and purity was checked using HPLC. ¹³C NMR spectra were recorded in Bruker FT 300 spectrometer. ESI Mass spectra were obtained by Micromass Quattro LC mass spectrometer. Purity of final product was determined in Varian ProStar HPLC at 210 nm with a flow rate of 1 mL/min in Varian microsorb 100-10 BDS reverse phase column (4.6 mm × 250 mm); mobile phase is methanol.

Antibodies

Caspase 3 (ab44976), Mdm2 (ab 38618), p-Mdm2 were purchased from Abcam, Cambridge, UK; BAX (PA5-17806), Bcl-2 (MA5-14937), Akt-1 (MA5-14898), p-Akt (ser 473, PA1-14032), STAT3 (PA5-16187), p-STAT3 (ser727, PA1-14393) goat anti-rabbit IgG alkaline Phosphatase conjugated (31340) were purchased from pierce protein research, USA; p53(#2524), Cytochrome C were purchased from Cell Signaling Technology, USA; VE-cadherin (sc-9989), secondary antibody mouse anti-rabbit IgG-FITC (sc-2359), and Texas Red-conjugated goat anti-mouse were purchased from Santa Cruz Biotechnology, USA.

Synthesis and characterization Dex derivative

Synthesis of tert-butyl-N-[2-(didecylamino)ethyl]-carbamate, compound C10a

tert-Butyl-*N*-(2-aminoethyl)carbamate (1 g, 6.25 mmol), potassium carbonate (3.45 g, 25 mol), and 1-bromodecane (3.45 g, 15.62 mmol) were dissolved into 25 mL dry ethyl acetate in a 50 mL round-bottom flask fitted with reflux condenser. The resulting mixture was refluxed over an oil bath at 70–80 °C for 48 h. Then reaction mixture was cooled, excess ethyl acetate was driven out by rotovac, and chloroform was added to this mixture. The whole mixture was transferred into a 500 mL separating funnel then it was

washed with water (3 × 100 mL) followed by brine (3 × 100 mL). The organic layer was dried with anhydrous sodium sulfate, filtered, and the solvent from the filtrate was removed by rotary evaporation. The mixture was purified by column chromatography using 60–120 mesh silica gel and 5% ethyl acetate hexane (v/v) as eluent yielded compound **C10a** as a yellowish liquid (1.65 g, 60% yield, $R_f = 0.75$ in 30% ethyl acetate hexane, v/v).

^1H NMR (400 MHz, CDCl_3): $\delta/\text{ppm} = 0.82\text{--}0.92$ [t, $J = 6.7$ Hz, 6H, $-\text{N}(-\text{CH}_2-\text{CH}_2-(\text{CH}_2)_7-\text{CH}_3)_2$], 1.23–1.33 [m, 28H, $-\text{N}(-\text{CH}_2-\text{CH}_2-(\text{CH}_2)_7-\text{CH}_3)_2$], 1.36–1.46 [m, 13H, $-\text{NH}-\text{CO}-\text{O}-\text{C}(\text{CH}_3)_3$, $-\text{N}(-\text{CH}_2-\text{CH}_2-(\text{CH}_2)_7-\text{CH}_3)_2$], 2.34–2.43 [t, $J = 7.4$ Hz, 4H, $-\text{N}(-\text{CH}_2-\text{CH}_2-(\text{CH}_2)_7-\text{CH}_3)_2$], 2.46–2.52 [t, $J = 6.4$ Hz, 2H, $-\text{CH}_2-\text{CH}_2-\text{NH}-\text{CO}-\text{O}-\text{C}(\text{CH}_3)_3$], 3.07–3.17 [m, 2H, $-\text{CH}_2-\text{CH}_2-\text{NH}-\text{CO}-\text{O}-\text{C}(\text{CH}_3)_3$].

Synthesis of (2-tert-butoxycarbonylamino-ethyl)-bis-decyl-methyl-ammonium iodide, compound **C10b**

Compound **C10a** (1 g, 0.21 mmol) was dissolved in 8 mL methyl iodide (MeI) in a 25 mL round-bottom flask, then potassium carbonate (K_2CO_3) (1.2 g, 0.82 mmol) was added. The resulting solution was stirred for 12 h at room temperature. Then reaction mixture was filtered, concentrated, and the residue was purified by column chromatography using 60–120 mesh silica gel and 6–7% methanol–chloroform (v/v) as eluent yielded compound **C10b** as a yellowish liquid (0.82 g, 80% yield, $R_f = 0.4$ in 10% methanol–chloroform, v/v).

ESI-MS: $m/z = 446$, (calculated value for $\text{C}_{28}\text{H}_{59}\text{N}_2\text{O}_2 = 445.6$).

Synthesis of compound **C10c**

Compound **C10b** (0.7 g, 0.57 mmol) was dissolved in 15 mL of dry DCM in a 25 mL round-bottom flask and stirred in an ice bath for 15 min. Then 7.5 mL of trifluoroacetic acid (TFA) was added drop wise to the solution. The resulting solution was further stirred in an ice bath for 2 h. The reaction mixture was transferred in 50 mL chloroform. Excess TFA was removed by washing with saturated sodium bicarbonate solution (3 × 100 mL). The organic layer was filtered, filtrate was dried over anhydrous sodium sulfate, and the solvent from the filtrate was removed by rotary evaporation. Evaporation of the organic layer afforded compound **C10c** as a reddish gummy material (0.518 g, 95.0% yield, $R_f = 0.1$, 10% methanol–chloroform, v/v). As compound **C10c** was obtained almost 90% pure (revealed by TLC), it was directly used for the next step.

Synthesis of compound **2**

Synthesis of compound **2** was done following the earlier described method [20]. Briefly, Dexamethasone (0.32 g, 0.83 mmol) was dissolved in ethanol (55 mL) and Water (25 mL) mixture followed by the addition of sodium periodate (0.21 g, 1.0 mmol) and 2 M sulfuric acid (1.7 mL) into a 250 mL round-bottom flask with continuous stirring at room temperature overnight. Then excess ethanol was removed and Water (25 mL) and brine (15 mL) were added to the reaction mixture. The pH of the solution was adjusted using 1 M aqueous sodium hydroxide to dissolve the product in solution. The mixture was then washed with DCM (3 × 60 mL) and then pH of the solution was adjusted to 3 with 1 M aqueous sodium bisulfate and finally extracted using ethyl acetate (2 × 100 mL) and 1:1 DCM:ethyl acetate (2 × 100 mL). These organic extracts were combined and dried with sodium sulfate and concentrated to get white solid compound **2**. (0.28 g, 97.0% yield, $R_f = 0.6$ in 10%, methanol–chloroform v/v).

^1H NMR (300 MHz, CDCl_3): $\delta/\text{ppm} = 0.92\text{--}0.97$ [d, $J = 7.1$ Hz, 3H, C_{20}H], 1.11 [s, 3H, C_{18}H], 1.20–1.30 [m, 2H, C_{15}H], 1.33–1.54 [m, 2H, C_7H], 1.56 [s, 3H, C_{19}H], 1.63–1.93 [m, 2H, C_{12}H], 2.0–2.22 [m, 1H, C_{14}H], 2.26–2.50 [m, 2H, C_6H], 2.50–2.76 [m, 1H, C_8H], 2.92–3.07 [m, 1H, C_{16}H], 3.3–3.38 [m, 1H, C_{11}H], 6.08 [s, 1H, C_4H], 6.21–6.33 [d, $J = 10.1$ Hz, 1H, C_2H], 7.27–7.39 [d, $J = 10$ Hz, 1H, C_1H].

ESI-MS: m/z 379, 401 [$\text{M}+\text{Na}^+$] (calculated value for $\text{C}_{21}\text{H}_{27}\text{FO}_5 = 378.43$).

Synthesis of compound **3**

Compound **2** (0.4 g, 0.53 mmol) was dissolved in 10 mL of dry dichloromethane (DCM) in a 50 mL round-bottom flask and stirred in an ice bath for 15 min. To this, a mixture of 1-ethyl-3-(3-dimethylaminopropyl)carbodiimide (EDCI) (0.164 g, 0.53 mmol) and Hydroxybenzotriazole (HOBt) (0.142 g, 0.52 mmol) was added, and stirring was continued for another 30 min. Then compound **C10c** (0.375 g, 0.57 mmol) was dissolved in 2 mL of dry DCM and added to the reaction mixture. Diisopropylethylamine (DIPEA) was added dropwise to the reaction mixture at ice cold condition (under stirring condition) until it became slightly basic. The resulting mixture was stirred for 18 h. Then the reaction mixture was dissolved in 30 mL chloroform, washed sequentially with water (3 × 30 mL), 1 N HCl (2 × 30 mL), saturated NaHCO_3 solution (3 × 30 mL), and brine (3 × 30 mL). The organic layer was dried with anhydrous sodium sulfate, filtered, and the solvent from the filtrate was removed by rotary evaporation. Then the residue was purified by column chromatography (using >200 mesh

silica gel and 3% methanol–chloroform (v/v) as eluent), followed by chloride ion exchange chromatography (using Amberlite IRA-400Cl resin and methanol as eluent) and yielded compound **3** (named as **DX10**) as a brown gummy solid (0.215 g, 25.0% yield, $R_f = 0.6$ in 10% methanol–chloroform (v/v)).

¹H NMR (300 MHz): δ /ppm = 0.84–0.93 [m, 9H, $J = 6.7$ Hz, $-N(-CH_2-CH_2-(CH_2)_7-CH_3)_2$, $C_{20}H$], 1.02 [s, 3H, $C_{18}H$], 1.14–1.39 [m, 33H, $-N(-CH_2-CH_2-(CH_2)_7-CH_3)_2$, C_7H , $C_{19}H$], 1.52–1.97 [m, 10H, $-N(-CH_2-CH_2-(CH_2)_7-CH_3)_2$, C_8H , $C_{12}H$, $C_{14}H$, $C_{15}H$], 1.99–2.85 [m, 7H, $-N(-CH_2-CH_2-(CH_2)_7-CH_3)_2$, C_6H , $C_{16}H$], 3.14 [s, 3H, $-OC-HN-CH_2-CH_2-N-CH_3$], 3.19–3.41 [t, 2H, $J = 6.7$ Hz, $-OC-HN-CH_2-CH_2$], 3.49–3.99 [m, 3H, $-OC-HN-CH_2-CH_2$, $C_{11}H$], 6.0 [s, 1H, C_4H], 6.22–6.29 [d, $J = 10.1$ Hz, 1H, C_2H], 7.46–7.56 [d, $J = 10.1$ Hz, 1H, C_1H], 8.0 [$-OC-NH-CH_2-CH_2$].

¹³C NMR (75 MHz, $CDCl_3$): δ /ppm = 186.8, 174.2, 167.1, 154.1, 129.1, 124.6, 102.0, 87.5, 70.9, 61.9, 61.5, 61.0, 48.0, 43.9, 36.1, 35.0, 34.3, 32.9, 32.6, 31.7, 31.0, 29.5, 29.3, 29.1, 29.0, 26.2, 22.9, 22.5, 22.2, 16.9, 15.8, 13.9.

ESI-MS: m/z 715.

ESI-HRMS = 715.5779 (calculated value for $C_{44}H_{76}N_2O_4F = 715.5783$).

HPLC purity = 97.8%.

Samples preparation and treatment

All compounds such as, DX10, WP, and Dex were dissolved in cell culture grade DMSO to get a primary stock. Then stocks were progressively diluted with DMSO to make secondary stock. Finally working concentrations of these compounds were obtained by adding the secondary DMSO stocks in 10% fetal bovine serum (FBS) containing cell culture medium. The concentration of DMSO into 10% FBS-containing working medium never exceeded more than 1%. For the cell viability studies an amount of 100 μ L of cell culture solution containing respective concentrations of derivatives was added to each well of 96-well plates and a few wells were kept untreated. For quantification of apoptosis and cell cycle studies an amount of 1.5 mL culture medium containing respective concentration of compounds were added to each well of the 6-well plates. For western blot studies B16F10 cells were cultured in T25 cell culture flask and 3–4 mL of cell culture medium containing respective concentrations of compounds were added.

Cell culture

B16F10 (murine melanoma), MCF7 (human breast adenocarcinoma), A549 (human lungs carcinoma), SKOV3 (human ovarian carcinoma), CHO (Chinese hamster

ovary), and NIH3T3 cell lines were purchased from the American Type Cell Culture (ATCC, USA) and National Center for Cell Sciences (Pune, India). All cells were cultured into mycoplasma-free condition. Cells were cultured in DMEM supplemented with 10% US origin FBS (Lonza, USA), 50 μ g/mL penicillin, 50 μ g/mL streptomycin, and 100 μ g/mL kanamycin at 37 °C humidified incubator injected with 5% CO_2 in air. Cultured healthy cells of 75–85% confluency were used for experiments. For cell plating, cells were first trypsinized, counted, and seeded into 6-well plates for quantification of apoptosis studies, and 96-well plates for cell viability studies. The cells were generally left overnight to adhere onto plates or flasks before they are used for experiments.

Cytotoxicity study

Cytotoxicity assay of the tested compounds were determined by the reduction of 3-(4,5-dimethylthiazol-2-yl)-2,5-diphenyltetrazolium bromide (MTT). Briefly, cells were plated in 96-well plates with density of 5000 cells/well usually 12–18 h before experiment. All compounds were mixed with DMEM to obtain required concentrations. These solutions were added to 96-well plates with at least triplicate wells. Treatments were carried out continuously for all types of cells with different time points. Following termination of treatment, cells were washed with phosphate buffer saline (PBS) and incubated with MTT solutions containing complete media at 37 °C for 4 h. Then media was discarded and MTT reduced violet crystals were dissolved in 50% DMSO/methanol solutions. Finally, the color was estimated using microplate reader at 550 nm wavelength. Results were represented as percentage of viability = $\{[A550 \text{ (treated cells)} - \text{background}]/[A550 \text{ (untreated cells)} - \text{background}]\} \times 100$.

Isobologram construction

Isobologram was constructed following previously illustrated protocol [23, 24]. Briefly, concentration of DX10 (IC_x, DX10) needed to produce cellular growth inhibition effect, x (e.g., 50% cell death) and the concentration of WP (IC_x, WP) required to produce same growth inhibition effect \times were plotted on the X- and Y-axis, respectively. The points of IC_x DX10 and IC_x WP were added by a straight line to produce the isobologram. After that, the junction in the same isobologram where the concentrations of individual component ($C_{DX10, X}$ & $C_{WP, X}$), used in combination treatment to produce the similar effect (x), were placed is called combination index (CI). CI value was calculated with the help of isobologram using the following equation.

$$CI = C_{DX10, X/ICx, DX10} + C_{WP, X/ICx, WP},$$

where $CI < 1$, $CI = 1$, $CI > 1$ indicates synergism, additivity, and antagonism effect, respectively.

Western blot analysis

For this study, B16F10 cells were kept UT or treated with DX10 (20 μ M), WP (10 μ M), [DX10+WP] (20 + 10) μ M for continuously 48 h in 10% FBS-containing DMEM. Following treatment, whole cell lysates of UT and different treatment groups were prepared as follows: cells were lysed with 50 mM Tris-HCl, pH 7.4, 0.15 M NaCl, 1% Nonidet P-40, 0.5% sodium deoxycholate, and 0.1% SDS, which was premixed with 1X protease inhibitor cocktail and 2 mM Sodium vanadate. Cell lysates of UT and different treatment groups were run in SDS-PAGE gradient gel according to antigen's molecular weight, and then bands were transferred to polyvinylidene fluoride (PVDF) membrane. BCIP/NBT was used for the development of protein bands by colorimetric method.

Glucocorticoid receptor (GR) down-regulation

Glucocorticoid receptor down-regulation was done using GR siRNA following previously described protocol [20]. Briefly, 2×10^5 B16F10 cells/well were plated in 6-well plates and incubated for 18 h. After that cells were either kept untreated or transfected with 40 pmol glucocorticoid receptor siRNA (Santa Cruz Biotech) and 40 pmol of scrambled siRNA (Qiagen) (diluted to 50 μ L with serum-free DMEM) using 4 μ L Lipofectamine 2000 (Invitrogen) (diluted to 50 μ L with serum-free DMEM). After 4 h of incubation, another 2 mL of complete DMEM media was added and incubated for another 20 h. Following of which, cells were harvested, counted, and again plated in 6-well plates at a 2×10^5 cells/well density for western blot analysis and cells were further plated at a 5000 cells/well density in 96-well plates for MTT study. For MTT study, after 12 h of incubation, cells were treated with different treatment groups and incubated for 48 h. After that MTT assay was performed following the above-mentioned protocol. For western blot study, after 12 h of incubation, cells were either kept untreated or treated with 20 μ M DX10, 10 μ M WP, and (20 + 10 μ M) [DX10+WP] for 36 h. After 36 h cells were lysed after that western blot analysis (as described earlier) was carried out for STAT3 and p-STAT3 along with GR to confirm the GR down-regulation.

GR siRNA (Santa Cruz Biotech): It is a pool of three different siRNA duplexes:

- a. GGCUUCAGGUAUCUUAUGATT
UCAUAAGAUACCUGAAGCCTT

- b. CCAAGAGCUAAUUUGAUGAATT
UUCAUCAAUAGCUCUUGGTT
 - c. CCAAGAGCUAAUUUGAUGAATT
UUCAUCAAUAGCUCUUGGTT
- Control siRNA** (Qiagen Inc.)
UUCUCCGAACGUGUCACGUTT
ACGUGACACGUUCGGAGAATT

IL-6 quantification

5×10^5 B16F10 cells were seeded in T25 flask. 18 h after incubation, cells were either kept untreated or treated with 5 μ M DX10, 20 μ M DX10, 10 μ M WP, (5 + 10 μ M) [DX10+WP], and (20 + 10 μ M) [DX10+WP] for 36 h. After that conditioned medium was collected and counted. The conditioned medium was then immediately processed for the IL6 measurement using mouse-specific IL6 ELISA kit (eBioscience) according to the manufacturer's instructions. The optical density was measured at 450 nm using microplate reader. The results were represented as graph of pg/mL in 10^6 cells.

Quantification of apoptosis study

Annexin V-FITC-labeled apoptosis detection kit (Sigma) was used to detect and quantify apoptosis by flow cytometry as per the manufacturer's instructions. Briefly, cells (2×10^5 cells/well) were seeded in 6-well plates and cultured overnight in 10% serum supplemented complete medium. After 16–18 h cells were either kept UT or treated with different concentrations of drugs for required time courses. Then the cells were harvested and collected by centrifugation for 5 min at 1000g. Cells were then resuspended at a density of 1×10^5 cells/mL in 1X binding buffer and stained simultaneously with FITC-labeled annexin V (25 ng/mL) and propidium iodide (50 ng/mL). Cells were analyzed using a flow cytometer (FACSCanto II), and data were analyzed with FACSDivaTM software. Minimum of 10,000 events were gated per sample.

Cellular DNA content measurements

Cells (2×10^5 cells/well) were seeded in 6-well plate for 12 h, then they were either kept UT or treated with DX10, WP, and [DX10+WP] over different time periods. Following that, cells of UT or different treatment groups were harvested, washed with 1X PBS, and fixed with 70% ethanol for 30 min at 4 $^{\circ}$ C. The resulting cells were centrifuged to discard ethanol and cell pellets were resuspended in 1X PBS. After centrifugation, cells were suspended in 1 mL of PI staining solution (40 μ g/mL propidium iodide, 0.1 mg/mL RNase, 0.05% Triton X-100) and kept in dark for 40 min at 37 $^{\circ}$ C. Next, cells were

collected by centrifugation, washed with 1X PBS, resuspended in 1 mL PBS, and analyzed using a flow cytometer (FACSCanto II, Becton Dickinson, San Jose, CA, USA). The data were analyzed with FACSDiva™ software. A minimum of 10,000 events were gated per sample and represented as histogram mentioning the percentage of cells in different phases of cell cycle.

Preclinical study in B16F10-based tumor model and quantification of apoptosis

To estimate tumor growth inhibition efficiency of [DX10+WP], we injected B16F10 cells to the right flank of the female C57BL6/J mice with 2.0×10^5 cells/mice. After 12 days of tumor cells inoculation mice of similar tumor volume were grouped for UT or treatment of WP, DX10, and [DX10+WP]. Maximum tolerance dose (MTD) of DX10 was pre-determined and exactly half of MTD was used for the treatment, i.e., 7.5 mg/kg with respect to body weight. Four injections (I.P.) were given every alternative day, and one injection was given in a gap of two days. For WP administration, we used variable doses so as to compare tumor growth regression effect, if any, in between WP and [DX10+WP] treatment. For this, 1st, 4th, and 5th doses were given with 15 mg/kg and 2nd, 3rd doses were given with 10 mg/kg WP with respect to mice body weight [25]. Hence combination doses of [DX10+WP] treatment was chosen accordingly. Compounds' stock solutions were prepared in DMSO solution and injected medium was 30% PEG and 0.5% NP-40 containing PBS, wherein DMSO concentration was less than 5%. Same blank solution was injected to UT grouped mice. On 24th day from tumor inoculation mice were humanly euthanized and tumors were isolated, cryosectioned, and analyzed for immunohistochemical studies. All animal work was conducted under protocols approved by Institutional Animal Ethical Committee of CSIR-IICT, India.

TUNEL assay and VE-cadherin staining

Isolated tumors were frozen in Jung tissue freeze medium (Leica Microsystem, Germany) followed by these being cryosectioned into 10 μ m thin using Leica CM1850 cryostat (Germany). The sections were fixed in 4% formalin in PBS for 15 min and TUNEL assay was done using DeadEnd fluorometric TUNEL assay kit (Promega, Madison, WI) as per manufacturer's protocol. The same cryosections were again stained using blood vessel staining marker (VE-cadherin primary antibody). For antibody staining, all tissue sections were washed and incubated with VE-cadherin mouse monoclonal antibody at 1:100 dilutions with 2% FBS in PBS

solutions for 2 h at 4 °C. After that, sections were washed with 1X PBS (3×10 min) and incubated with Texas Red-conjugated goat anti-mouse secondary antibody with 1:500 dilutions into same buffer for 45 min at 4 °C. After completion of secondary antibody incubation, slides were washed with 1X PBX (3×10 min). Images were acquired under Nikon TE2000E inverted fluorescence microscope at 10 \times magnification using required filters.

Estimation of p-STAT3 expression in tumor sections

Tumor sections of UT and treated mice groups were analyzed for estimating expression of p-STAT3 (ser 727), which is responsible for drug resistance in cancer cells. For this experiment, 10 μ m thin tumor sections of treated and untreated mice were first incubated with anti-p-STAT3 (ser727) rabbit monoclonal antibody (pierce protein research, USA) at a dilution of 1:100 in 2% FBS in PBS for 2 h at 4 °C. Following this, washing with PBS, same sections were incubated with FITC-conjugated goat anti-rabbit secondary antibody at dilution of 1:500 into 2% FBS in PBS for 1 h at 4 °C. Then repeat washing step and sections were visualized under Nikon TE 2000E microscope at 10X magnification under green channel fluorescence.

Statistical analysis

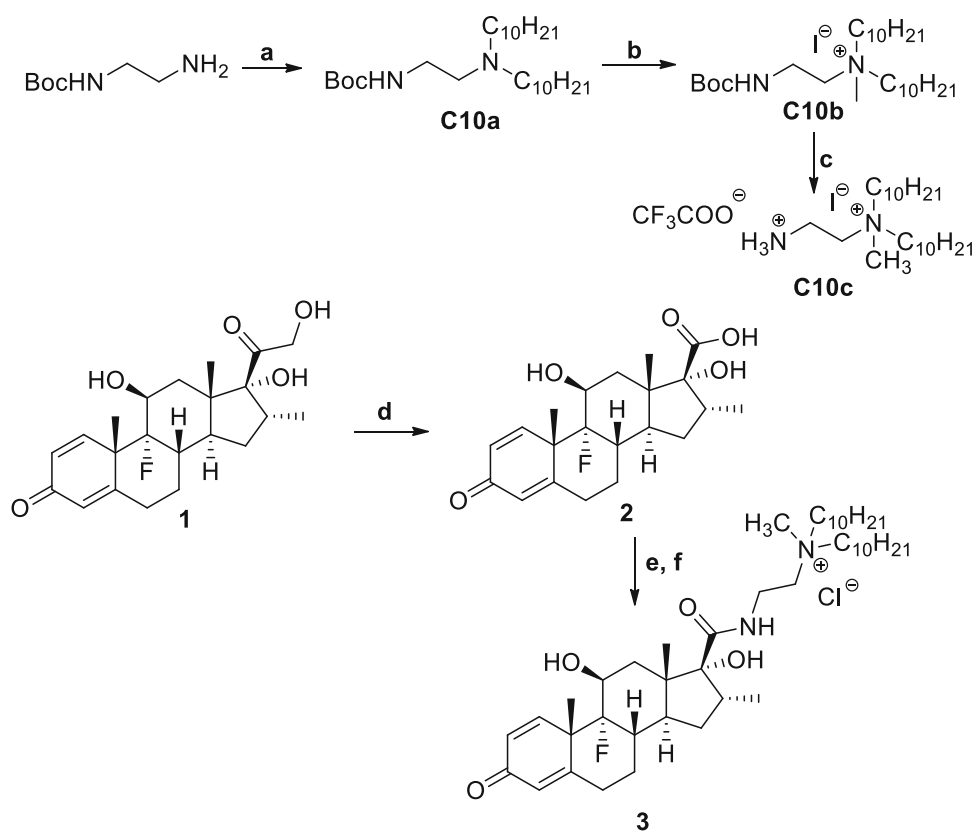
Data were expressed as the mean SD and statistically analyzed by the two-tailed, unpaired, Student's t-test using Microsoft Excel (Seattle, WA). For animal studies, scores were considered significant when $p < 0.05$. For in vitro studies, scores were considered significant when $p < 0.01$.

Results

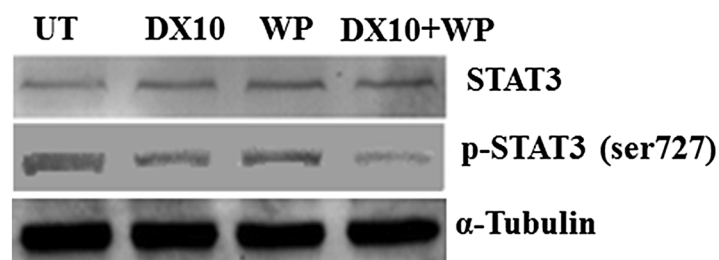
Synthesis of Dex derivative

Here we synthesized ten carbon long cationic chain conjugated Dex derivative by chemically conjugating ten carbon long cationic twin chain in the 17-position of Dex following previously established protocol with slight modification [20]. Briefly, first amine group of *tert*-butyl-*N*-(2-aminoethyl)carbamate was reacted with 1-bromodecane to obtain ten carbon long chain containing tertiary amines (**C10a**). This was further quaternized using methyl iodide to produce BOC-protected quaternized amine (**C10b**). BOC deprotection was done using trifluoroacetic acid to obtain free amine compound (**C10c**). On the other hand, Dex was oxidized by NaIO₄ to obtain free carboxylic acid functionality containing compound

Scheme 1 Synthesis of DX10. Reagents and conditions: **a** 1-bromodecane, K_2CO_3 , EtOAc, 70–80 °C, 48 h; **b** methyl iodide, dry DCM, K_2CO_3 , 12 h; **c** trifluoroacetic acid (TFA): DCM (1:2), 2 h; **d** $NaIO_4$, H_2SO_4 , H_2O , EtOH, overnight stirring; **e** EDCI, HOBT, DIPEA, dry DCM, 18 h; **f** amberlite IRA 400Cl, methanol



A



B

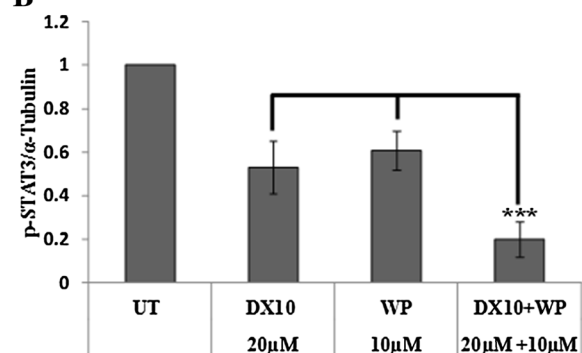
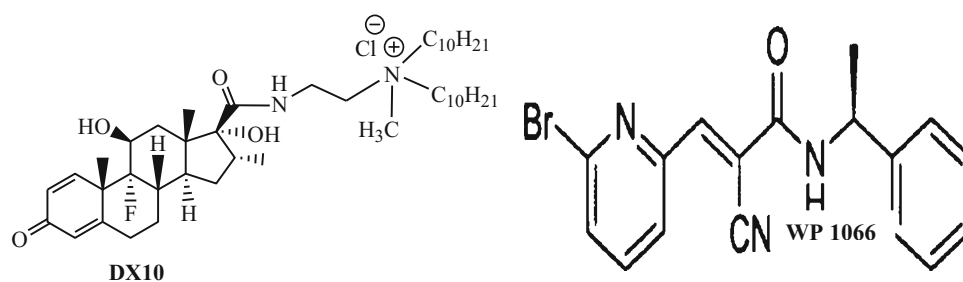


Fig. 1 a STAT3 and p-STAT3 (ser 727) protein expression level in B16F10 cells after 36 h of continuous treatment with DX10 (20 μ M), WP (10 μ M), [DX10+WP] (20 + 10 μ M). UT denotes the untreated

group. **b** Densitometry-based quantification (*bar plots*) of p-STAT3 (ser 727) normalized with respect to α -Tubulin. The asterisk (***) indicates $p < 0.001$

Scheme 2 Structures of newly DX10 and commercially available JAK/STAT3 inhibitor, WP



2; then this acid compound **2** was coupled with free amine group of ten cationic long containing quaternary amines (**C10c**) in the presence of EDCI, DIPEA in DCM. Finally, the resultant amide was passed through ion exchange resin (Amberlite IRA 400Cl) to obtain the final product in the chloride form, compound **3** (**DX10**). The detailed synthetic scheme is delineated in Scheme 1. Scheme 2 indicates the chemical structure of DX10 and WP1066.

[DX10+WP] treatment down regulates p-STAT3 activation

Following DX10 preparation we have checked the STAT3 inhibitory activity of DX10 to establish the hypothesis that DX10 might also possess STAT3 inhibitory activity just like DX8 [20]. Additionally here we have used WP along with DX10 to amplify the STAT3 inhibitory activity (if any) of DX10. The results (Fig. 1a) show that 36 h of

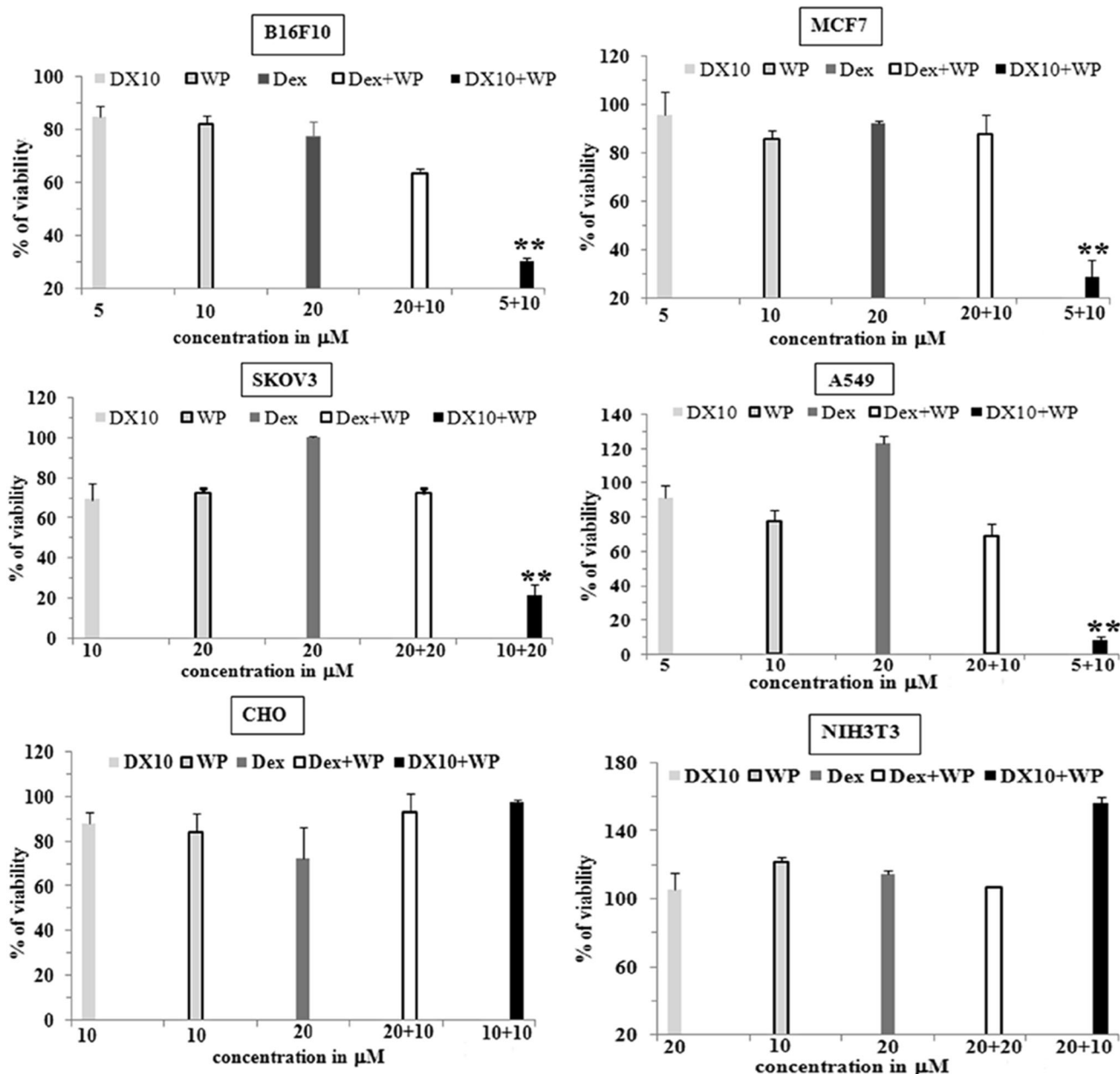


Fig. 2 Cell viability studies in B16F10, MCF7, A549, SKOV3, CHO, and NIH3T3 cell lines following continuously treatment with DX10, WP, Dex, [Dex+WP], and [DX10+WP] with given

concentration (mentioned in X-axis) for 48 h. The asterisk (**) indicates $p < 0.001$ of [DX10+WP] with respect to DX10, WP, and [Dex+WP]

treatment with DX10, WP, and (DX10+WP) did not change STAT3 expression. However, the p-STAT3 expression is significantly down-regulated in combination treatment as compared to either DX10 or WP treatment. Almost seven-fold reduction in p-STAT3 expression is quantified for (DX10+WP) treatment, whereas only 2.5–3-fold p-STAT3 expression is reduced either of the individual treatment as compared to UT group (Fig. 1b). Thus this study proves our preliminary hypothesis and also preferably supports the combination use of DX10 with WP towards inhibiting the STAT3 activation.

DX10 and WP combination treatment induces synergistic effect on cancer cell growth

Towards utilizing the p-STAT3 inhibitory effect on cellular viability, we opted to carry out the cytotoxicity study of DX10 and WP individually or combination of DX10 and WP in different cancer cell lines, such as B16F10, MCF-7, A549, SKOV3, and in non-cancer cell lines such as CHO and NIH-3T3 (Fig. 2). We included Dex for both individual treatment or in combination with WP. Firstly, we standardized the optimum concentration of all individual and combination treatments after several trials using a range of concentration. For individual treatments of Dex, WP, and DX10, we chose those concentrations where these molecules have little effect of cytotoxicity. In contrast, combination treatment of [DX10+WP] at this concentration induces significantly higher killing in cancer cells. However, Dex and WP combination didn't have much impact on toxicity when compared with [DX10+WP] effect. Interestingly, co-treatment of DX10 with WP imparts cytotoxicity in cancer cells but not in non-cancer cells. Next to check whether this combination treatment produces any synergism anti-cancer activity, we have constructed Isobologram (Fig. S1) following previously established method [23, 24]. From this plot we find that the combination index (CI) values are less than one for all tested cancer cells which prove the synergistic effect of the DX10 and WP when they are used together.

DX10 individually and in combination with WP exerted GR-mediated anti-cancer effect by stopping IL6 release

As DX10 is a cationic lipid modified derivative of dexamethasone, a synthetic ligand for glucocorticoid receptor (GR), we hypothesized that GR may have a role in DX10 mediated synergistic effect. Consequently to investigate the role of GR, we studied the effect of different treatment groups on p-STAT3 protein

expression level after silencing GR. For that, B16F10 cells were treated either with GR siRNA or with scrambled siRNA (Sc siRNA), then both set of cells were either kept untreated (UT) or respectively treated with DX10 (20 μ M), WP (10 μ M), and [DX10+WP] (20 + 10 μ M) continuously for 36 h. We found that in scrambled siRNA (Sc siRNA) treated cells were experienced significant inhibition of p-STAT3 in DX10 treated group (Fig. 3b). However, with GR siRNA-treated set of cells, where GR was clearly down-regulated, were not experienced any appreciable amount of inhibition in p-STAT3 by DX10 treated group. As expected the effect of WP remains same in both set of cells as far as inhibition of STAT3 activation is concerned. The inhibition of STAT3 activation by combination treatment of DX10 and WP was increased by twofold in Sc siRNA-treated cells when compare to GR siRNA-treated cells (Fig. 3d). This established that GR is essential for DX10 to inhibit the STAT3 activation.

Further, we studied the involvement of GR on DX10 (either alone or in combination with WP) induced cellular toxicity as evident in Fig. 2. For this, GR siRNA and Sc siRNA-treated B16F10 cells were exposed respectively with DX10 (5 μ M), WP (10 μ M) and DX10+WP (5 + 10 μ M). For better comparison the concentration of individual treatment groups were kept similar to what was used in cellular viability study (Fig. 2). We found that, DX10 exhibited slightly better cytotoxicity towards Sc siRNA pre-treated cells (71% viable cells) compare to that of GR siRNA pre-treated cells (83% viable cells). However, cytotoxicity effect of (DX10+WP) treatment diminished by 2.5 fold in GR siRNA-treated cells (48% viable cells) compare to that of Sc siRNA-treated cells (19% viable cells). Collectively these two studies (Fig. 3a–e, Fig. S3) support the fact that GR is necessary for DX10-mediated effect (p-STAT3 inhibition and cellular toxicity) even in the combination treatment.

It is evident from the earlier literature study that GR has a potential role in IL6 mediated JAK-STAT pathway [26–29] and above experiment proves the involvement of GR in DX10 mediated inhibition of STAT3 activation. Therefore, the effect of DX10 either alone or in combination with WP in the formation IL6 was investigated in B16F10 cells. For this study, B16F10 cells were either kept untreated (UT) or respectively treated with different treatment groups for 36 h, after which the conditioned medium was collected and IL6 amount was measured (Fig. 3f). IL6 amount in conditioned medium of 5 μ M and 20 μ M DX10 treated B16F10 cells were found to be 56 and 38 pg/mL, respectively, which showed a dose-wise decrement compare to that of untreated group (82 pg/mL). Further, 10 μ M WP treatment lowers the IL6 amount by

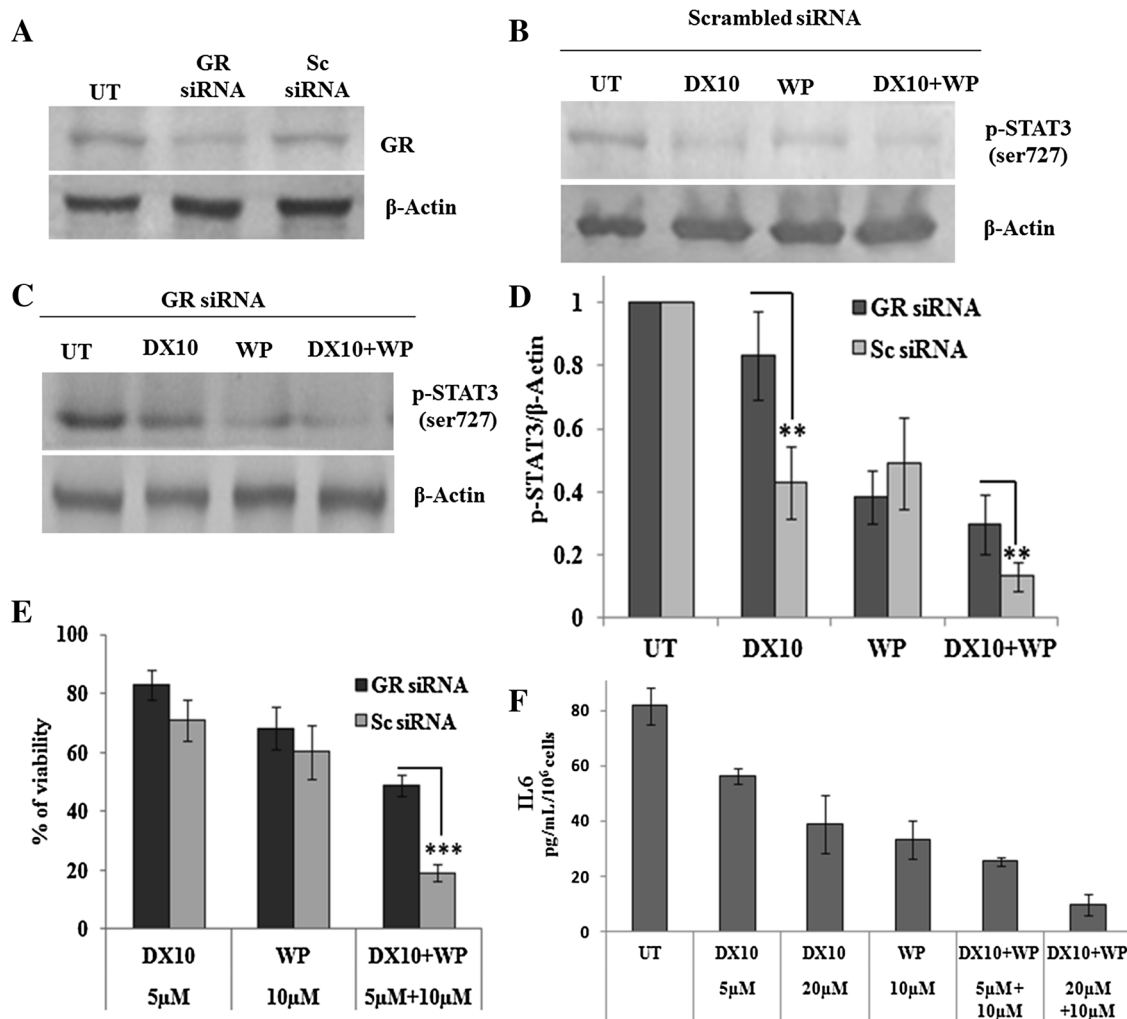


Fig. 3 **a** GR expression levels in B16F10 cells: cells were either untreated (UT) or respectively treated with GR siRNA (40 pmol) (GR siRNA), or treated with scrambled siRNA (40 pmol) (Sc siRNA) for 72 h. **b** p-STAT3 (ser727) protein expression levels in cellular lysates of **b** scrambled siRNA-treated B16F10 cells or **c** GR siRNA-treated B16F10 cells following treatment with 20 μM DX10, 10 μM WP, and (20 + 10 μM) [DX10+WP] for 36 h. **d** Quantification of the p-STAT3 band normalized with respect to β-actin. **e** Cellular viability study of the GR siRNA or Sc siRNA-treated B16F10 cells after

treatment with indicated treatment groups. **f** Quantitative representation of IL6 amount present in the conditioned medium of B16F10 cells following 36 h of respective treatment with 5 μM DX10, 20 μM DX10, 10 μM WP, (5 + 10 μM) [DX10+WP] and (20 + 10 μM) [DX10+WP]. UT represents IL6 amount present in the conditioned medium of untreated cells. IL6 amount is represented as pg of IL6 present in each mL of conditioned medium obtained from 10⁶ cells. The asterisk (**) and (***) represent $p < 0.01$ and $p < 0.001$ respectively

58% when compared to the UT group. However, combination treatment of 5 and 20 μM DX10 with 10 μM WP showed 68 and 88% reduction in IL6 amount respectively when compared to the UT group. This study proves that reduction of IL6 by DX10 treatment may be the plausible reason for inhibition of STAT3 activation and subsequent cell death.

Co-treatment of DX10 and WP induces apoptosis in cancer cells

Selective cytotoxicity and synergistic effect of [DX10+WP] treatment in cancer cells may be associated

with induction of apoptosis. Therefore to ascertain the induction of apoptosis by the combination treatment, we have used dual marker Annexin V-FITC/propidium iodide (PI) based apoptosis assay using flow cytometer. The result shows (Fig. 4) that co-treatment of DX10 and WP induces increased amount of early stage apoptosis in B16F10 cells (lower right quadrant, 42.3%), whereas individual treatment groups had little effect in B16F10 cells (with 16.7 and 20.4% of early apoptosis in the WP and DX10 treated cells respectively). The summary of apoptosis in B16F10 and CHO cells has been provided in Fig. S2. However, combination or independent treatment did not induce any significant amount of apoptosis

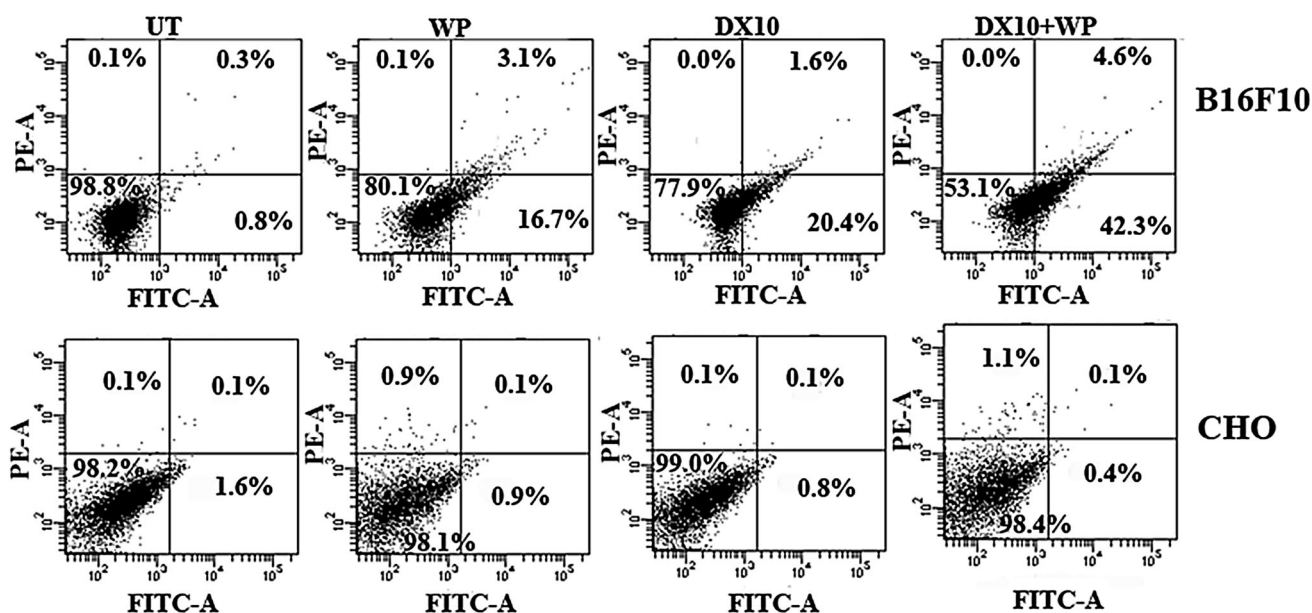


Fig. 4 Flow cytometric estimation of apoptosis in B16F10 (28 h treatment) and CHO (48 h treatment) cells either kept UT or treated with 5 μ M of WP, 10 μ M of DX10, (10 + 5) μ M of [DX10+WP]. In [DX10+WP] treatment in B16F10 cells induces higher percentage of

early apoptosis compared to UT, WP, and DX10. Contrastingly, CHO is remained unaffected with the treatment of [DX10+WP] even at 48 h

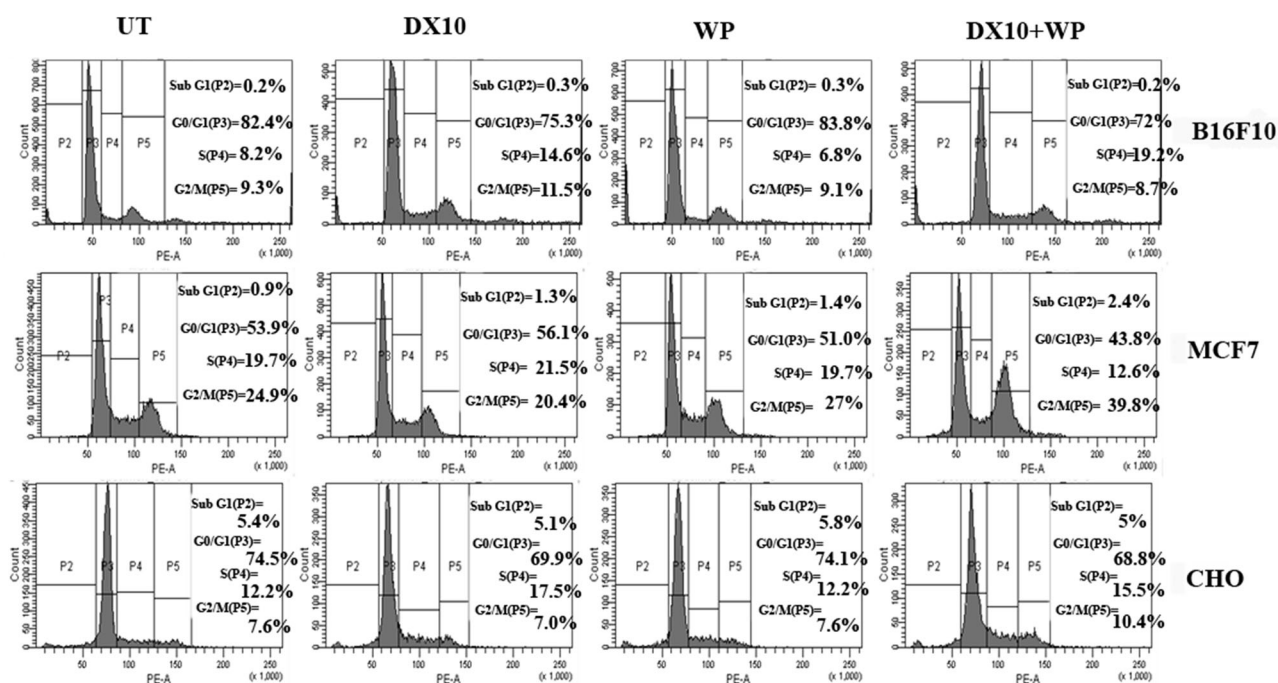


Fig. 5 Flow cytometric analysis of cell cycle in B16F10 (upper panel), MCF-7 (middle panel), and CHO cells (lower panel) using propidium iodide (PI). Cell-populations in different phases were mentioned in right part of each histogram

in normal cell like CHO when compare to the untreated group. Thus, co-treatment of DX10 and WP selectively induces early stage apoptosis in B16F10 but not in CHO cells.

Effect of DX10 and WP co-treatment in cell cycle

To compare the distribution pattern of cells in different phase of the cell cycle following combinational treatment

or individual treatment, we performed PI binding assay based DNA content measurement using flow cytometer. Herein, B16F10, MCF7 and CHO cell lines were either kept UT or treated with DX10, WP, [DX10+WP] with variable concentration. From Fig. 5, it is clear that B16F10 cells treated with (10 + 5) μM of [DX10+WP] for 36 h has higher population at S-phase (P4) (19.2%) than that of UT (8.2%) or other treated groups (14.6 and 6.8% for DX10 and WP-treated cells, respectively). However, MCF7 cells treated with (5 + 5) μM of [DX10+WP] for 24 h showed selective G2/M-phase (P5) arrested profile. Contrastingly, (10 + 5) μM of [DX10+WP] treated for 48 h in CHO cells didn't show any significant cell cycle arrest in any phase when compare to the untreated group. Thus, the combination treatment of DX10 and WP causes multimodal way of cell cycle arrested profile selectively in cancer cells but not in non-cancer cells. Arresting of more cancer cells in a particular phase of a cell cycle with combination treatment when compare to other treatment groups endorse the synergistic effect of the combination treatment.

[DX10+WP] activates pro-apoptotic factors

Apoptosis operates through two major processes, one is intracellular stimulatory pathway (intrinsic pathway) and another is death receptor signaling mediated (extrinsic pathway). This process of apoptosis is executed by Bcl-2 family proteins and mitochondrial effectors [30]. The Bcl-2 family proteins consist of both pro- as well as anti-apoptotic subtypes determines the propensity toward the program cell death. This Bcl-2 family protein promotes irreversible translocation of mitochondrial effector protein Cytochrome C to cytoplasm and thereby activates Caspase-protease cascade such as Caspase 3. This process promotes cells to undergo apoptosis. Figure 6 indicates that [DX10+WP] treatment in B16F10 cells significantly increases the BAX/Bcl-2 protein ratio; almost 4 and 1.3 times compare to DX10 and WP-treated groups respectively. Resultant increment of BAX/Bcl-2 ratio in the combination treatment enhances the Cytochrome C release from mitochondria to cytoplasm and followed with

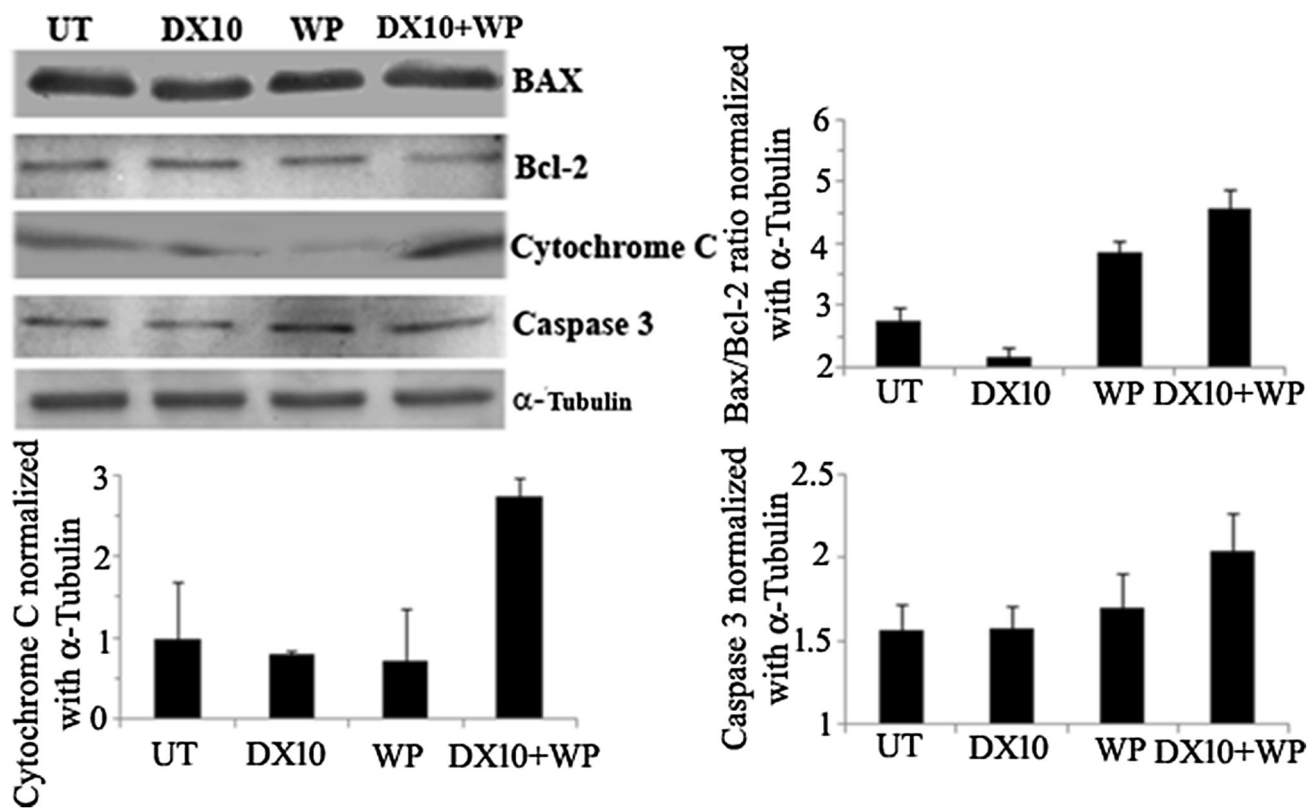


Fig. 6 Western blot analysis and quantification (bar plots) of ratio between BAX and Bcl-2, Cytochrome C and Caspase 3. The quantification of bands were done through normalization of individual bands with respect to α -Tubulin. For this experiments B16F10 cells

were either kept untreated (UT) or respectively treated with DX10 (20 μM), WP (10 μM), [DX10+WP] (20 + 10) μM for 36 h continuously. The data indicates that combination treatment of [DX10+WP] up-regulates apoptotic regulatory factors significantly

caspase-3 up-regulation which leads to early apoptotic event. Thus, co-treatment of DX10 and WP drives more B16F10 cells in the early apoptotic phase and thus more cellular growth arrest (Fig. 1) as compare to either of the treatment groups.

[DX10+WP] treatment activates p53 to induce apoptosis through reduction of Akt expression

The process of apoptosis manifests with the balance of cellular stress signals and survival pathways. The vital tumor suppressor protein (p53) responds to various stress signals such as DNA damage, hypoxia and oncogene suppression. Thus, p53 is committed to induce apoptosis.

In cancer, serine/threonine kinase such as Protein Kinase B (Akt) plays important role for cell survivability by blocking cell death stimuli and inhibiting the process of apoptosis [31]. Therefore, p53 and Akt play in opposite direction and they determine a cell to induce apoptosis or survivability.

The activation of p53 is closely regulated by oncoprotein Mdm2 which generally activated by p-Akt. Activated p-Mdm2 stabilizes the formation of p53-Mdm2 complex and thereby helps sequestration of p53 activity in response to stress. Therefore, in order to understand the cross-talk in between p53-Akt and Mdm2, we performed western blot analysis of lysates, obtained from B16F10 cells treated with DX10, WP and [DX10+WP]. We found [DX10+WP] treatment significantly reduce Akt expression and

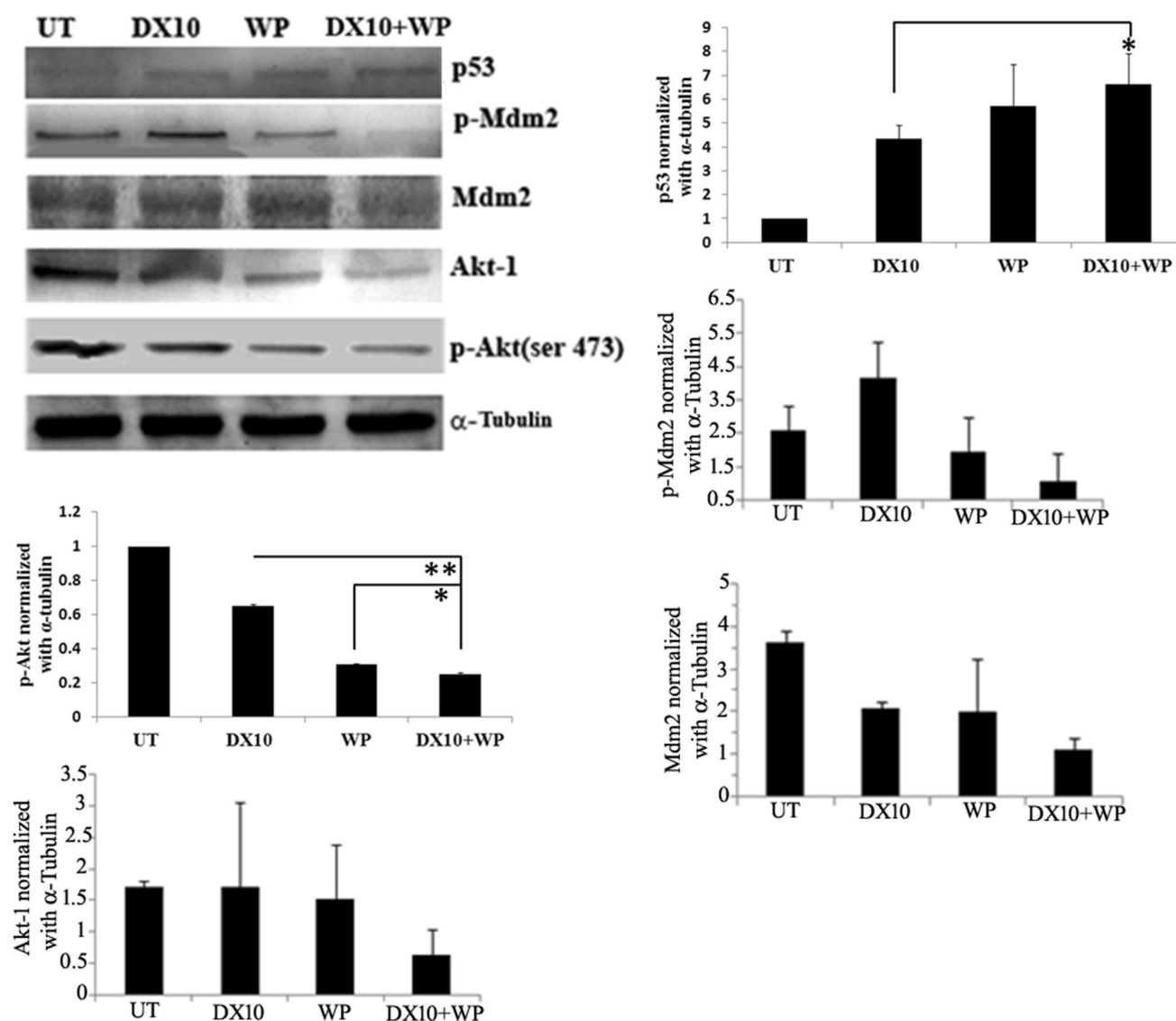


Fig. 7 Western blot analysis and densitometry-based quantification (bar plots) of p53, p-Mdm2, Mdm2, Akt-1, P-Akt (ser 473) and α -Tubulin proteins bands. All bands were quantified and normalized with respect to loading control such as α -Tubulin. B16F10 cells were

either kept UT or respectively treated with DX10 (20 μ M), WP (10 μ M), [DX10+WP] (20 + 10) μ M for 36 h continuously. The asterisk (*) and (**) denoted $p < 0.01$ and 0.001 respectively

consequently reduction of p-Akt (Fig. 7). The reduction of Akt expression stops Mdm2 from being converted to p-Mdm2 and thus no loss of p53 from ubiquitination which otherwise resulted from p53-Mdm2 complex formation [20]. Figure 7 collectively demonstrated that cancer cell killing by [DX10+WP] is mediated through up-regulation of tumor suppressor protein p53 and down-regulation of cell survival kinases, Akt.

Effect of [DX10+WP] on tumor regression and in induction of apoptosis in tumor cells and tumor associated endothelial cells

Since, [DX10+WP] treatment induced synergistic killing, apoptosis and cell cycle arrest selectively in cancer cells; therefore, we were keen to observe anti-tumor effect of [DX10+WP] in B16F10 cell-based highly aggressive

murine melanoma model. In this study, from day 12 (after B16F10 cell inoculation) onwards to total five injections were given with DX10, WP, DX10+WP and one group of mice were kept untreated. The result (Fig. 8a) shows that DX10+WP combination treatment exhibited maximum tumor growth inhibition. However, DX10 and WP were also inhibited tumor growth, but in lesser volume compare to their combination treatment. On day 24th after tumor cell inoculation, average tumor size grew for DX10 or WP-treated mice almost twofold more compare to that of DX10+WP-treated group mice. Figure 8b demonstrates the representative tumor pictures from each group, isolated after termination of experiment.

Tumor regression study exhibited that combination treatment have maximum tumor growth inhibition. As growth of angiogenic vessel of tumor tissue is necessary for the growth of tumor, we thought that induction of

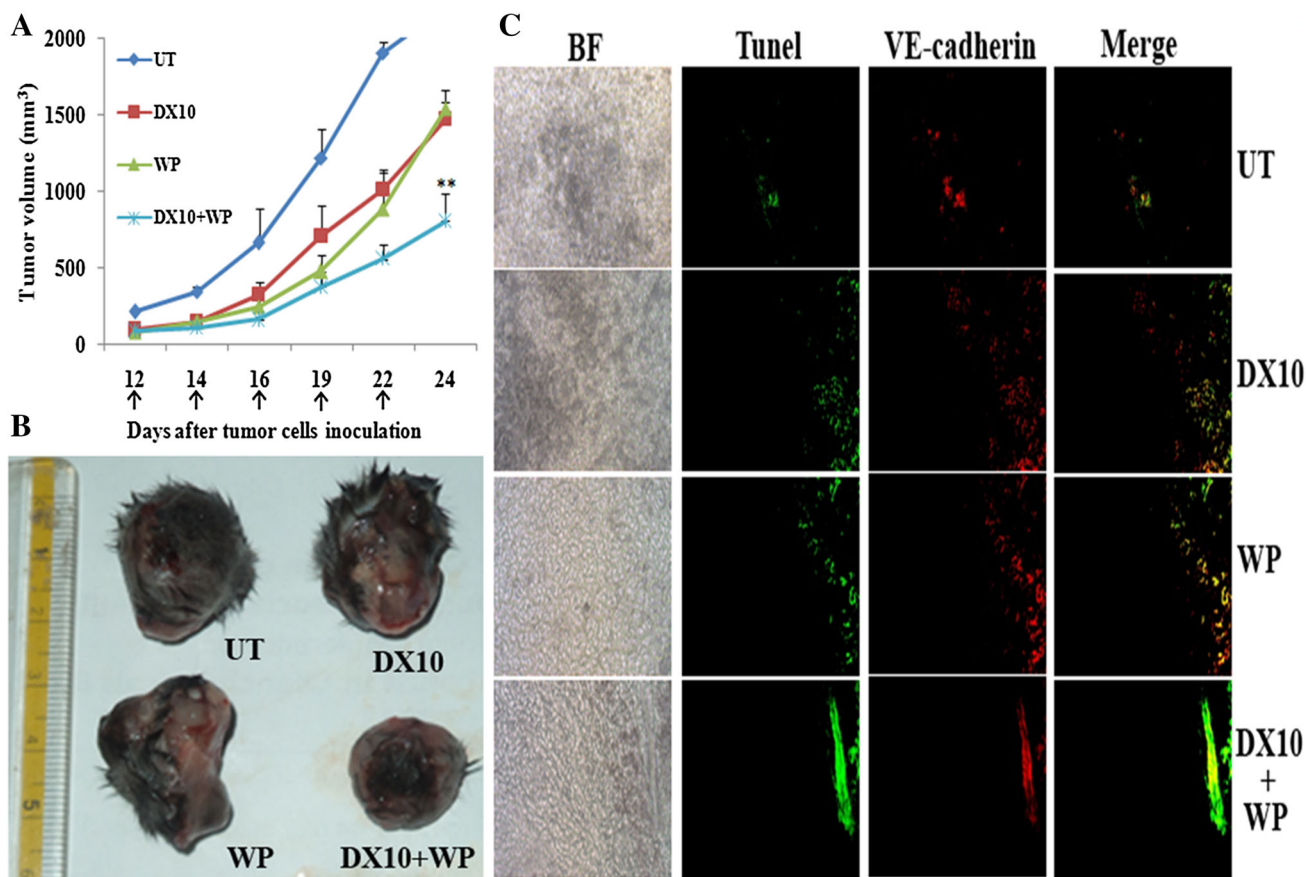


Fig. 8 a In vivo tumor regression study using B16F10 cell-based melanoma model. Mice were either kept UT or injected (I.P) with DX10, WP, [DX10+WP]. The days of injection were as indicated by black arrow in X-axis. During the course of dosing, UT mice group was separated from the other treatment group due to uncontrolled tumor growth. The asterisk (**) indicates $p < 0.05$ for [DX10+WP] with respect to DX10 and WP treatment, respectively. **b** Representative tumor pictures of different treatment and UT groups, isolated after termination of experiment (days on 24th). **c** Microscopic pictures

of 10 μ m tumor sections obtained from UT (first row), DX10 (second row), WP (third row), and DX10+WP (fourth row) treated mice group. Starting from left, first column indicates the tissue architecture in bright field (BF), second indicates apoptotic regions obtained from TUNEL assay (green fluorescent), third is endothelial regions stained with VE-cadherin antibody (red fluorescent), and extreme right indicates merge image picture respectively. All the images were acquired at $\times 20$ magnification using respective filters of inverted fluorescence microscopy. (Color figure online)

apoptosis in the angiogenic vessel by DX10+WP treatment may be the possible reason behind this potent anti-tumor activity. Thus here we carry out the TUNEL assay to find out the apoptosis induction activity of different treatment groups both in tumor tissue and its angiogenic vessel. For this study, tumors of UT and all treated mice group was isolated and cryosectioned. After that, tumor sections were stained using green fluorescence-based TUNEL assay for detection of apoptosis. Additionally, the same tissue sections were stained with endothelial cells marker VE-cadherin, (using VE-cadherin primary antibody) for detection of angiogenic endothelial cells.

From Fig. 8c, it is clear that the [DX10+WP]-treated tumor section contains more apoptotic areas (i.e., more green fluorescence) compared to that in tumor sections obtained from UT, WP, DX10-treated mice. Merge panel of [DX10+WP]-treated tumor section shows there are higher level of yellow color, which indicates the induction of apoptosis in vascular endothelial cells. Thus, it is clear that tumor section of combination treatment, [DX10+WP] exhibited considerable amount of apoptosis in both tumor cells and tumor associated endothelial cells.

Combination treatment of DX10 and WP downregulates p-STAT3 in tumor tissue

In vitro studies showed that DX10, WP and their combination treatment inhibit STAT3 activation, with combination treatment having the maximum inhibitory effect. Thus to evaluate the p-STAT3 inhibitory effect of combination treatment in vivo, we check p-STAT3 level in the tumor cryosection, obtained from mice treated with different treatment groups, using immunohistochemical assay. For this, tissue sections were stained with p-STAT3 primary antibody and leveled with FITC-conjugated secondary antibody. Figure 9 shows significant down-regulation of p-STAT3 (ser 727) (green region) level in [DX10+WP]-treated mouse tumor than the UT or DX10- and WP-treated one. Consistent to the in vitro result, WP and DX10 treatment also block STAT3 activation in the tumor compare to UT group. Collectively, in vivo study demonstrate that combination treatment holds melanoma tumor growth by inhibiting STAT3 activation and inducing apoptosis in tumor mass and its angiogenic vessels.

Discussion

Dexamethasone (Dex), a synthetic ligand for glucocorticoid receptor, is commonly used along with chemotherapy to alleviate side effects of the chemotherapy [15–17]. However, repeated use of Dex

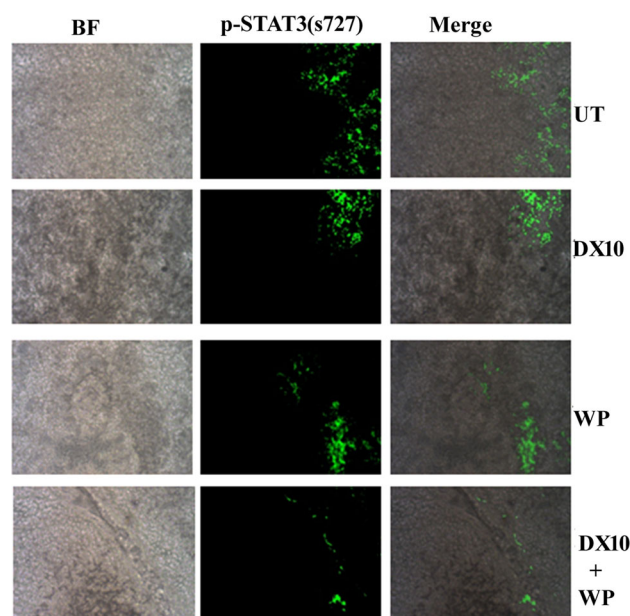


Fig. 9 Microscopic pictures of 10 μ m tumor sections, obtained either from UT (first row) or DX10 (second row), WP (third row), and [DX10+WP] (fourth row) treated mice group. Tissue sections are represented as first column from left is bright field (BF), second column from left is p-STAT3 (ser727) antibody stained (green fluorescence), and third column from left is merge, respectively. (Color figure online)

frequently resulted with drug resistivity [19]. On the contrary Dex is also known to work against lymphoid malignancies and hormone refractory cancer [15, 32]. Mixed results of pristine Dex propelled us to modify Dex such a way that modified Dex bestows with uniform anti-cancer activity. Towards this in our recent study [20] we developed cationic Dex which showed selective anti-cancer activity by inhibiting STAT3 activation. This result brought us the idea of using cationic Dex along with another potent STAT3 inhibitor to enhance the anti-tumor activity of cationic Dex by synergistically inhibiting STAT3 which plays important roles for many cancers. Therefore, in the current study we developed a new cationic Dex (DX10) by chemically conjugating Dex with ten carbon cationic twin long chain and resultant DX10 inhibits STAT3 activation. Then with a view to increase the STAT3 inhibition effect WP1066 is used along with DX10. We indeed find that this combination strategy resulted in more p-STAT3 inhibitory effect compared to either of the treatment groups. Next, to find out that if this STAT3 inhibitory activity is actually leading to any cell death or not, we carried out viability study and it is observed that combination treatment synergistically kills cancer cells but not non-cancerous cells.

As Dex exerted its activity through GR, here we questioned that DX10 might also be working in the same way.

To answer this GR siRNA study was done, where we find that DX10 either as alone or in combination with WP is working through GR. JAK/STAT3 activity is generally monitored by IL-6 cytokine [26–29]. On the other hand, some literature suggested that IL-6 production is inhibited by Dex through its receptor GR [33]. Thus GR may play an indirect role towards maintaining JAK/STAT3 activity. Previously Obrador et al., reported that GR-knocking down (using GR siRNA) causes down-modulation of IL-6 release in B16-melanoma cells [34]. Therefore it could be expected that GR siRNA pre-treated cells could show the down-modulation of IL-6 in DX10+WP treatment. In this regard, we check the IL-6 status and find out that IL-6 amount clearly decreased in all DX10 treatment. However, reduction of IL-6 by Dex treatment (much lesser extent compare to DX10) doesn't lead to similar extent of p-STAT3 inhibitory effect (data not shown). The mechanistic study proves that combination treatment arrests the cell in different phases of the cell cycle followed by induction of early apoptosis and finally cell death. Since this new combinational strategy shows its efficacy in vitro, thus to extrapolate and validate the result we carried out in vivo study. Where combination treatment inhibits tumor growth significantly and blocks the STAT3 activation in tumor lesion, which is fully consistent with our in vitro observation.

Conclusion

To summarize, in the current study we have developed a new combination chemotherapeutic using novel DX10 and WP which showed potent anti-cancer activity through synergistic inhibition of p-STAT3. Activity of DX10 is GR mediated and this combination treatment induces early apoptosis. Findings from melanoma tumor study proved the synergistic therapeutic benefit where DX10+WP inhibit tumor growth through simultaneous induction of apoptosis and inhibition of STAT3 activation. Taken together, the presently reported combination treatment evokes immense possibilities in development of anti-tumor therapeutics, particularly against cancer where STAT3 serves as an important oncoprotein.

Acknowledgements SS and SKM thank Council of Scientific and Industrial Research (CSIR), Government of India, New Delhi for their doctoral research fellowships. RB acknowledges financial assistance from CSIR Network Project Grant [CSC0302, BSC0123], Govt. of India.

Compliance with ethical standards

Conflict of interest The authors declare that there is no conflict of interest.

References

- Gottesman MM (2002) Mechanisms of cancer drug resistance. *Annu Rev Med* 53:615–627
- Vogelstein B, Papadopoulos N, Velculescu VE, Zhou S, Diaz LA, Kinzler KW (2013) Cancer genome landscapes. *Science* 339:1546–1558
- Housman G, Byler S, Heerboth S, Lapinska K, Longacre M, Snyder N, Sarkar S (2014) Drug resistance in cancer: an overview. *Cancers* 6:1769–1792
- O'Shaughnessy J, Osborne C, Pippen JE, Yoffe M, Patt D, Rocha C, Koo IC, Sherman BM, Bradley C (2011) Iniparib plus chemotherapy in metastatic triple-negative breast cancer. *N Engl J Med* 364:205–214
- Amadori D, Cecconetto L (2006) Gemcitabine and taxanes in metastatic breast cancer. *Ann Oncol* 17:173–176
- Rocha LC, Sherman CA, Brescia FJ, Brunson CY, Green MR (2001) Irinotecan/gemcitabine combination chemotherapy in pancreatic cancer. *Oncology* 15:46–51
- Akira S (1999) Functional roles of STAT family proteins: lessons from knockout mice. *Stem Cells* 17:138–146
- Garcia R, Bowman TL, Niu G, Yu H, Minton S, Muro-Cacho CA et al (2001) Constitutive activation of Stat3 by the Src and JAK tyrosine kinases participates in growth regulation of human breast carcinoma cells. *Oncogene* 20:2499–2513
- Gouilleux-Gruart V, Gouilleux F, Desaint C, Claisse JF, Capiod JC, Delobel J et al (1996) STAT-related transcription factors are constitutively activated in peripheral blood cells from acute leukemia patients. *Blood* 87:1692–1697
- Fernandes A, Hamburger AW, Gerwin BI (1999) ErbB-2 kinase is required for constitutive stat 3 activation in malignant human lung epithelial cells. *Int J Cancer* 83:564–570
- Simonian PL, Grillot DA, Nuñez G (1997) Bcl-2 and Bcl-XL can differentially block chemotherapy-induced cell death. *Blood* 90:1208–1216
- Kunigal S, Lakka SS, Sodadasu PK, Estes N, Rao JS (2009) Stat3-siRNA induces Fas-mediated apoptosis in vitro and in vivo in breast cancer. *Int J Oncol* 34:1209–1220
- Alas S, Bonavida B (2003) Inhibition of constitutive STAT3 activity sensitizes resistant non-Hodgkin's lymphoma and multiple myeloma to chemotherapeutic drug-mediated apoptosis. *Clin Cancer Res* 9:316–326
- Herr I, Ucur E, Herzer K, Okouoyo S, Ridder R, Krammer PH et al (2003) Glucocorticoid cotreatment induces apoptosis resistance toward cancer therapy in carcinomas. *Cancer Res* 63:3112–3120
- Rutz HP (2002) Effects of corticosteroid use on treatment of solid tumours. *Lancet* 360:1969–1970
- Rutz HP, Herr I (2004) Interference of glucocorticoids with apoptosis signaling and host-tumor interactions. *Cancer Biol Ther* 3:715–718
- Kriegler AB, Bernardo D, Verschoor SM (1994) Protection of murine bone marrow by dexamethasone during cytotoxic chemotherapy. *Blood* 83:65–71
- Harousseau JL, Attal M, Leleu X, Troncy J, Pegourie B, Stoppa AM et al (2006) Bortezomib plus dexamethasone as induction treatment prior to autologous stem cell transplantation in patients with newly diagnosed multiple myeloma: results of an IFM phase II study. *Haematologica* 91:1498–1505
- Sui M, Chen F, Chen Z, Fan W (2006) Glucocorticoids interfere with therapeutic efficacy of paclitaxel against human breast and ovarian xenograft tumors. *Int J Cancer* 119:712–717
- Sau S, Banerjee R (2014) Cationic lipid-conjugated dexamethasone as a selective antitumor agent. *Eur J Med Chem* 83:433–447
- Ferrajoli A, Faderl S, Van Q, Koch P, Harris D, Liu Z et al (2007) WP1066 disrupts Janus kinase-2 and induces caspase-dependent

- apoptosis in acute myelogenous leukemia cells. *Cancer Res* 67:11291–11299
22. Iwamaru A, Szymanski S, Iwado E, Aoki H, Yokoyama T, Fokt I et al (2007) A novel inhibitor of the STAT3 pathway induces apoptosis in malignant glioma cells both in vitro and in vivo. *Oncogene* 26:2435–2444
 23. Tallarida RJ (2001) Drug synergism: its detection and applications. *J Pharmacol Exp Ther* 298:865–872
 24. Chou TC (2010) Drug combination studies and their synergy quantification using the Chou-Talalay method. *Cancer Res* 70:440–446
 25. Kong LY, Abou-Ghazal MK, Wei J, Chakraborty A, Sun W, Qiao W et al (2008) A novel inhibitor of signal transducers and activators of transcription 3 activation is efficacious against established central nervous system melanoma and inhibits regulatory T cells. *Clin Cancer Res* 14:5759–5768
 26. Takeda T, Kurachi H, Yamamoto T, Nishio Y, Nakatsuji Y, Morishige KI et al (1998) Crosstalk between the interleukin-6 (IL-6)-JAK-STAT and the glucocorticoid-nuclear receptor pathway: synergistic activation of IL-6 response element by IL-6 and glucocorticoid. *J Endocrinol* 159:323–330
 27. Zhang Z, Jones S, Hagoood JS, Fuentes NL, Fuller GM (1997) STAT3 acts as a co-activator of glucocorticoid receptor signaling. *J Biol Chem* 272:30607–30610
 28. Verhoog NJ, Du Toit A, Avenant C, Hagoood JP (2011) Glucocorticoid-independent repression of tumor necrosis factor (TNF) alpha-stimulated interleukin (IL)-6 expression by the glucocorticoid receptor: a potential mechanism for protection against an excessive inflammatory response. *J Biol Chem* 286:19297–19310
 29. Nishimura K, Nonomura N, Satoh E, Harada Y, Nakayama M, Tokizane T et al (2001) Potential mechanism for the effects of dexamethasone on growth of androgen-independent prostate cancer. *J Natl Cancer Inst* 93:1739–1746
 30. Gross A, McDonnell JM, Korsmeyer SJ (1999) BCL-2 family members and the mitochondria in apoptosis. *Genes Dev* 13:1899–1911
 31. Gottlieb TM, Leal JF, Seger R, Taya Y, Oren M (2002) Crosstalk between Akt, p53 and Mdm2: possible implications for the regulation of apoptosis. *Oncogene* 21:1299–1303
 32. Nishimura K, Nonomura N, Satoh E, Harada Y, Nakayama M, Tokizane T et al (2001) Potential mechanism for the effects of dexamethasone on growth of androgen-independent prostate cancer. *J Natl Cancer Inst* 93:1739–1746
 33. Waage A, Slupphaug G, Shalaby R (1990) Glucocorticoids inhibit the production of IL 6 from monocytes, endothelial cells and fibroblasts. *Eur J Immunol* 20:2439–2443
 34. Obrador E, Valles SL, Benlloch M, Sirerol JA, Pellicer JA, Alcácer J, Coronado JAF, Estrela JM (2014) Glucocorticoid receptor knockdown decreases the antioxidant protection of B16 melanoma cells: an endocrine system-related mechanism that compromises metastatic cell resistance to vascular endothelium-induced tumor cytotoxicity. *PLoS ONE* 9(5):e96466